Dynamic determinations of the Grüneisen coefficient in aluminum and aluminum alloys for densities up to 6 Mg/m^3†

T. Neal
University of California, Los Alamos Scientific Laboratory, Los Alamos, New Mexico 87545
(Received 7 June 1976)

With the use of the Mie-Grüneisen equation, thermodynamic states off the principal Hugoniot are analyzed to obtain experimental results for the Grüneisen coefficient. Such states are achieved through the phenomena of regular and Mach reflection and through shock compression of porous samples whose initial densities are less than the standard density on which the principal Hugoniot is centered. Measurements of the speed of release waves in shocked material also permit the Grüneisen coefficient to be evaluated. The composite result for the dependence of the Grüneisen parameter on volume is compared with some functional forms commonly used in shock-wave work.

I. INTRODUCTION

There are three experimental curves which can serve as valuable references for the high-pressure equation of state of metals. The first is an isotherm, usually measured at room temperature. Useful isothermal results are limited, however, to the calibrated pressures that can be achieved by static methods. Dynamic "isentropic" compression by magnetic flux, for example, and approximate isentropic compression by a large number of small shocks are rather new fields of study. Although volumes can be determined directly, the high pressures must usually be inferred or calculated by numerical hydrodynamic techniques to match dynamic performance. Thus the chief reference at very high pressures remains the principal Hugoniot, the locus of all thermodynamic states attainable directly by shock compression from whatever are considered standard conditions for a particular metal. The outstanding problem then becomes how to describe thermodynamic states which are not on the principal Hugoniot. One of the simplest and most commonly used formulations is the Mie-Grüneisen equation, which relates pressure to internal energy and volume and has a theoretical basis which makes it useful for interpreting shock-wave results. The success of this approach has resulted partly from the Grüneisen coefficient for shocked materials being principally a function of volume and rather insensitive over much of the range of interest to internal energy or temperature. Knowledge of the volume dependence of this parameter is therefore the key to describing states off the principal Hugoniot. For some specific metals, attempts have been made to calculate the Grüneisen coefficient by means of assumed interatomic potentials.[1] Among the more generalized theories posed for calculating this parameter, that of Dugdale and MacDonald, that of Slater, and that which uses the free-volume approximation, have been more commonly applied in shock-wave work.[2] For some metals this question has been tackled experimentally by determining Hugoniots for porous samples. Since such additional Hugoniots are centered on below-standard densities, a Grüneisen coefficient can be evaluated from the difference between the several high-pressure references. These Hugoniots, however, always refer to states which have more specific energy than states of corresponding volume on the principal Hugoniot. In that case it sometimes becomes necessary to account for vaporization of the material or to distinguish between that portion of the pressure and energy supplied by lattice compression and that portion which is basically an electronic contribution. States with less energy than those on the principal Hugoniot may be investigated by multiple shocking of a metal to the desired volume. These relatively colder states can also be utilized to evaluate the Grüneisen coefficient with respect to the principal Hugoniot. In fact, very high compressions can be more easily achieved with multiple shocks because the thermal contribution to the pressure is much smaller.

In this paper some experimental determinations of the Grüneisen coefficient for aluminum and aluminum alloys will be presented. Although these materials have slightly different chemical compositions, there are sufficient other uncertainties in the experiments that no attempt will be made to distinguish between the final results on that basis. The measurement of bulk sound speeds in shocked materials will be reviewed first. These experiments determine the velocity of a release wave propagating into a region that has been shock compressed. Next the case of shocks reflecting from materials of higher impedance will be considered. Then the results of multiple shocks obtained by regular reflection will be reviewed and a new re-

sult obtained from a three-stage compression by regular reflection techniques will be described. Some old and new results for Mach reflection will also be included. Information gained from Hugoniot experiments on porous samples will also be introduced. Finally, the results for the Grüneisen coefficients obtained by all the various techniques will be compared with commonly used analytic forms for metals.

II. BULK SOUND SPEEDS

The bulk sound speed characterizes the lower limit of the speed with which very small disturbances, that is, weak shocks or relaxation waves, propagate through shock-compressed material. Measurements of sound velocity play a large part in the study of the equation of state. The Mie-Grüneisen equation of state is written with respect to the principal Hugoniot pressure and energy, P_i and E_i, as

$$P_i' - P_i = (E_i' - E_i)\gamma(V_i)/V_i \ . \tag{1}$$

The function $\gamma(V)$ is the Grüneisen coefficient and the convention of primed quantities, referring to values for a state at volume V_i that is not on the principal Hugoniot, is adopted. This equation can be solved in the acoustic limit to yield[3]

$$\gamma(V_1) = 2V_1\left[\left(\frac{\partial P_1}{\partial V_1}\right)_H - \left(\frac{\partial P_1'}{\partial V_1}\right)_S\right] \Big/ \left[P_1 + \left(\frac{\partial P_1}{\partial V_1}\right)_H (V_0 - V_1)\right] , \tag{2}$$

where V_0 is the volume on which the Hugoniot is centered, the derivative with subscript H is the slope of the Hugoniot at volume V_1, and that with subscript S is the slope of the isentrope which passes through P_1 and V_1. This latter derivative is related to C_1, the bulk sound speed of the material compressed to V_1, by

$$\left(\frac{\partial P_1'}{\partial V_1}\right)_S = \frac{-C_1^2}{V_1^2} \ . \tag{3}$$

Several measurements of the bulk sound speed in shock-compressed materials were made a number of years ago by Al'tshuler *et al.*[4] for pressures ranging from 41.2 GPa (412 kbar) to 196 GPa (1.96 Mbar). The experimental technique used was the overtaking-relaxation method.[5] In this technique a flying plate is impacted on a sample plate and shocks are induced in both. As the shock progresses through the sample, the shock in the flyer reaches the back surface and a rarefaction returns through the flyer plate and subsequently enters the sample. The location in the sample where the head of the plastic rarefaction overtakes the shock can be used to deduce the bulk sound speed of the shocked material. In practice the measurement of bulk sound speed reduces to the experimental determination of the shock-wave trajectory in the sample, plus a measurement of whatever parameters are necessary to specify the magnitudes of the shocks. The results of five experiments on aluminum and the Grüneisen coefficients, as calculated from Eq. (2) with the Soviet Hugoniot, are listed in the first five rows in Table I. The standard deviations for γ, listed in parentheses, correspond to 2% errors in the sound speeds. Since no experimental errors were quoted, these represent a guess as to the precision of this type of experiment. The first two values of γ disagree with the others. Curran[6] has pointed out that elastic effects probably caused erroneous measurements at the two lower pressures. The shock trajectories for those two were determined experimentally by a different method than the latter three. In any case, these two determinations of γ will be disregarded here.

Two bulk sound speed measurements in 1100-*F* aluminum obtained by the present author using a different experimental method were recently reported.[7] In those experiments a shock impinged obliquely on a free surface and the head of the reflected plastic rarefaction was observed radiographically. These results are listed at the end of Table I. The accompanying standard deviations illustrate a well-known fact. At low compressions the value of the Grüneisen coefficient is particularly sensitive to the sound speed. At this pressure a 1% uncertainty in the sound speed is reflected as a 30% uncertainty in γ. As can be seen from the previous results, at higher compressions this difficulty is not so serious. The reason for this is that the Grüneisen coefficient is proportional to the difference between the slope of the Hugoniot and the slope of the isentrope passing through the compressed state. In the limit of zero compression these slopes are identical. As the compression achieved by the shock is increased, the Hugoniot rapidly becomes steeper and these slopes normally differ more and more. Thus for small compressions γ depends on a small difference between two relatively large numbers, and a minor

TABLE I. Results of bulk sound speed measurements.

P_1 (GPa)	V_1 (Mg/m^3)	C_1 (km/sec)	$\gamma(V_1)$
41.2	0.280	8.13	0.86 (±0.48)
54.5	0.267	8.84	0.73 (±0.35)
97.5	0.241	9.76	1.39 (±0.18)
160.0	0.217	11.23	1.12 (±0.12)
195.5	0.210	11.74	0.98 (±0.11)
27.4 ± 1.2	0.297 ± 0.002	7.49 ± 0.10	1.21 ±0.48
27.7 ± 1.0	0.297 ± 0.001	7.45 ± 0.18	1.45 ±0.85

uncertainty in one of them can significantly affect that small difference. At higher compressions, as for example in Al'tshuler's highest compression experiment, a 2% error in the sound speed induced only an 11% error in γ. Thus bulk sound speed measurements can be very useful in determining the Grüneisen coefficient, but only at high compressions.

III. REFLECTED SHOCKS

A two-stage shock compression can be achieved by transmitting a shock through a sample and then reflecting the shock from a material of higher shock impedance. In metals, as a result of such a second compression, pressures behind the reflected shock can be up to several times as great as the incident pressure. The technique is analyzed graphically in Fig. 1 for the case of a shock passing from aluminum to copper. The solid lines are principal Hugoniots while the dotted lines represent second Hugoniots for aluminum, that is, Hugoniots centered on a state achieved by shock compression. The method illustrated at 30 GPa is analogous to the impedance-match technique used to collect principal-Hugoniot data. To obtain Hugoniot data for copper, some formulation for γ is assumed and the 30-GPa second Hugoniot for aluminum is calculated and taken as a reference. The initial density and the shock velocity are measured for the copper and a straight line with the slope of their product, $\rho_0 U_s$, is constructed through the origin. In Fig. 1 this line is dashed; its intersection with the aluminum second Hugoniot establishes a result on the principal Hugoniot of copper. To determine the Grüneisen coefficient, this approach can be inverted by considering the copper principal Hugoniot (preferably obtained by fundamental measurements) as the reference and using the shock velocity measurement to establish the pressure and particle velocity in the copper. The fact that the 30-GPa second Hugoniot for aluminum must pass through this point on the copper Hugoniot establishes a value of the Grüneisen coefficient. The drawback to this method is its lack of precision and accuracy. The dashed line of slope $\rho_0 U_s$ intersects the copper Hugoniot at such a small angle that any error or uncertainty is greatly magnified when determining the pressure. This in turn escalates the uncertainty in γ.

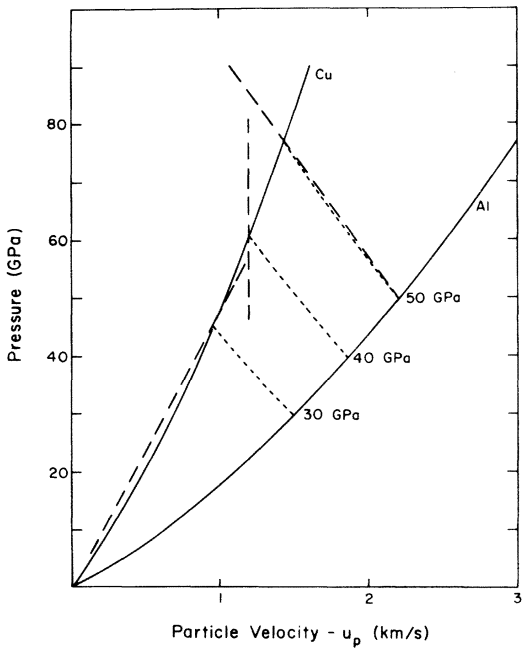

FIG. 1. Analyses of shocks in aluminum reflecting from copper. Solid lines are the reference principal Hugoniots. Dashed lines represent the graphical construction that would be used to determine the state in the copper for three different experimental methods. Dotted lines are the resulting recentered Hugoniots for aluminum.

A better method of determining γ is to measure the particle velocity in the copper. This approach is illustrated in the graphical construction for 40 GPa. The dashed line representing fixed particle velocity does not intersect the copper Hugoniot at such a small angle, and the effect of uncertainties is subsequently reduced. This method, however, does not work as well with high shock impedance materials since their Hugoniots in this plane rise so steeply that they again intersect lines of constant particle velocity at small angles. The most precise method for determining γ is illustrated in the 50-GPa example. In this case the velocity of the reflected shock in the aluminum is observed directly. A dashed line emanating from the 50-GPa result on the aluminum principal Hugoniot is constructed with slope $-U_{s_2}/V_1$, where U_{s_2} is the velocity of the reflected shock with respect to the material in front of it and V_1 is the volume in the aluminum achieved by the 50-GPa shock. This dashed line intersects the copper Hugoniot at an even larger angle than in the previous method. Direct measurement of the reflected shock, however, can probably only be accomplished with radiographic techniques or embedded signal gauges. Thus far this method has not received much application.

If two shocks of the same magnitude collide in a given material, there exists a plane of mirror symmetry which, for purposes of the flow description, is completely equivalent to a rigid wall—a hypothetical object representing the ultimate in shock impedance. If the collision angle α_1, the semiangle between the two shocks, does not exceed

a certain critical value, the phenomenon of regular reflection results and two reflected shocks occur. The actual pattern of shocks can be understood by examining the portion of Fig. 2(a) in which the angles are labeled. The reflection angle, one-half the angle between the reflected shocks, is denoted by β_1. The shock and particle velocities for the second shock are given by[7]

$$U_{s_2} = U_{s_1}(\sin\beta_1/\sin\alpha_1) + u_{p_1}\cos(\alpha_1+\beta_1) \tag{4}$$

and

$$u_{p_2} = u_{p_1}\cos\alpha_1/\cos\beta_1 . \tag{5}$$

The corresponding volume, pressure, and energy—which can be obtained from the Rankine-Hugoniot shock relations[2]—are

$$V_2 = V_1(1 - u_{p_2}/U_{s_2}) , \tag{6}$$

$$P_2' = P_1 + u_{p_2}U_{s_2}/V_1 = \rho_0 u_{p_1}U_{s_1} + u_{p_2}U_{s_2}/V_1 , \tag{7}$$

and

$$E_2' = E_1 + \tfrac{1}{2}(P_1 + P_2')(V_1 - V_2) . \tag{8}$$

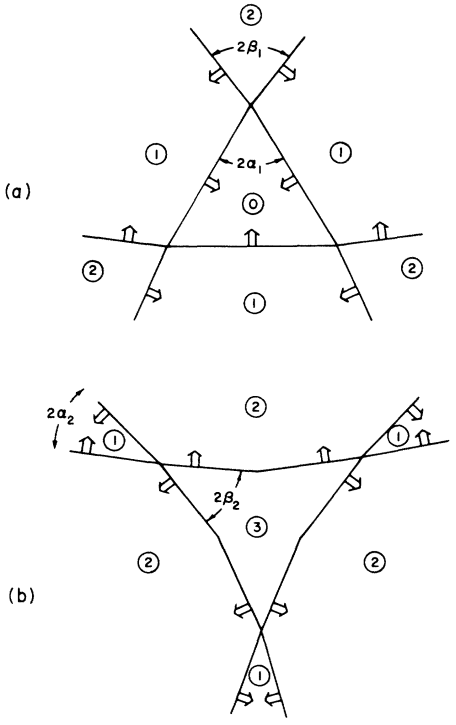

FIG. 2. Creation of double regular reflection. In (a) three cases of regular reflection occur as plane shocks converge toward the center. In (b), which represents the situation after convergence and at the time of radiography, three cases of double regular reflection are present. Small double arrows indicate the direction of motion of the shocks and the integers indicate the number of times material in that region has been shocked.

Here ρ_0 is the initial density and P_1, V_1, and E_1 refer to the state achieved by the incident shock. The convention for primed quantities is continued. Since P_2 and E_2, the pressure and energy of a state on the principal Hugoniot at volume V_2, are known, Eq. (1) can be used directly to evaluate γ.

Over a decade ago Al'tshuler and Petrunin[8] published a few results for symmetrical oblique collisions in which the angle α_1 was determined by experimental design and the angle β_1 was observed radiographically. Their single result for aluminum and the value of γ determined from it with the use of their Hugoniot are as follows:

$$\begin{aligned} &P_1 = 36 \text{ GPa}, \quad V_2 = 0.235 \text{ Mg/m}^3 , \\ &P_2' = 95.2 \text{ GPa}, \quad \text{and} \quad \gamma(V_2) = 1.34 \pm 0.52 . \end{aligned} \tag{9}$$

The standard deviation for γ corresponds to a 1.25° uncertainty assigned to β_1.

A three-stage compression may be achieved in a similar fashion using this same phenomenon. Three shocks are caused to converge as shown in Fig. 2(a). For the particular experiment to be discussed this system was chosen to have threefold rotational symmetry. The first collision angle, α_1, was therefore 30°. Over a wide range of shock strengths this collision angle results in regular reflection in most metals. The circled integers indicate the number of times material in that region has been shock compressed. As time elapses, the principal shocks will converge to the center and the original reflected shocks will themselves collide and cause regular reflection again as shown in Fig. 2(b). Region 3 thus represents material which has been shock compressed three times and α_2 and β_2 represent the angles for the second occurrence of regular reflection. For this experiment the two cases of reflection are related by

$$\alpha_2 = 60^\circ - \beta_1 . \tag{10}$$

Note that in all there are six secondary reflected shocks and six places where they intersect. Three of these intersections are at the second regular reflections just discussed. The other three result in a different type of interaction which is not shown in Fig. 2(b) but whose effects are minor and do not perturb the area of interest. Equations (4) and (5) describe the shock and particle velocities for the second case of regular reflection if all subscripts are simply incremented by one. The volume, pressure, and energy attained behind the second regular reflection are given by

$$V_3 = V_2(1 - u_{p_3}/U_{s_3}) , \tag{11}$$

$$P_3' = P_2' + u_{p_3}U_{s_3}/V_2 , \tag{12}$$

TABLE II. Results for regular reflection and double regular reflection.

ρ_0 (Mg/m^3)	2.70	α_1 (deg) [a]	30	α_2 (deg) [a]	$60° - \beta_1$
C_0 (km/sec)	5.24	β_1 (deg) [a]	36.49 ± 0.79	β_2 (deg) [a]	27.82 ± 0.28
S_0	1.40	U_{s_2} (km/sec)	9.24 ± 0.18	U_{s_3} (km/sec)	11.79 ± 0.58
U_{s_1} (km/sec) [a]	7.28 ± 0.07	u_{p_2} (km/sec)	1.57 ± 0.06	u_{p_3} (km/sec)	1.63 ± 0.07
u_{p_1} (km/sec)	1.46 ± 0.05	P_2' (GPa)	77.7 ± 4.1	P_3' (GPa)	155.8 ± 10.7
P_1 (GPa)	28.7 ± 1.3	V_2 (m^3/Mg)	0.246 ± 0.003	V_3 (m^3/Mg)	0.212 ± 0.003
V_1 (m^3/Mg)	0.296 ± 0.002	$\gamma(V_2)$	1.54 ± 0.20	$\gamma(V_3)$	1.11 ± 0.26

[a] Measured directly.

and

$$E_3' = E_2' + \tfrac{1}{2}(P_2' + P_3')(V_2 - V_3) . \quad (13)$$

Values of γ can be determined as before for both stages of compression.

An experimental test of this flow phenomenon used three 102-mm cubes of Composition B-3 explosive initiated with P-081 plane-wave lenses to induce shocks in a triangular 6061 aluminum prism. The faces of the sample contacting the explosive were 102-mm square. A matched explosive system was used to induce a shock in a separate sample where the velocity of the incident shock was measured with piezoelectric timing pins. In principle, both β_1 and β_2 should be measured at the time of convergence. In practice, β_2 cannot be measured just then since region 3 exists only as a point. Our experience with regular reflection has shown, however, that these angles vary sufficiently slowly with time that the angle should lie within the standard deviation of a measurement made when region 3 has expanded enough to permit the angle to be resolved. In this experiment β_1 was also measured at the same time as β_2 so that only one radiograph would be needed. The previous comment again applies. This led to some degradation in the precision of β_1 and in a more recent experiment on beryllium, a separate matched experiment was conducted to measure this angle at the time of convergence. The results of the aluminum experiment, which was radiographed with a 40-nsec pulse from the PHERMEX radiographic facility,[9] are listed in Table II. The quantities C_0 and S_0 refer to an empirical linear relationship between shock and particle velocity,

$$U_{s_1} = C_0 + S_0 u_{p_1} , \quad (14)$$

which describes the principal Hugoniot for this material. The final density achieved corresponds to a pressure on the principal Hugoniot of 198 GPa, almost seven times that of the incident pressure.

IV. MACH REFLECTION

When the collision angle α exceeds some critical limit, the phenomenon of regular reflection is superseded by that of Mach reflection. The resulting situation is shown in Fig. 3 for the case of a symmetrical collision. The confluence of the incident and reflected shocks is not attached to the mirror-image plane as in regular reflection but is joined to it by a shock known as a Mach stem which intersects the confluence at angle θ. Recently this flow has been analyzed successfully for shocks in solids by a modified version of the three-shock model with a slip line.[7] This model will be briefly reviewed here. In Fig. 3 a slip line is shown to emanate from the shock confluence at angle δ and the trajectory of the confluence diverges from the wall at a growth angle ϕ, which is assumed to be constant. The requirement that the Mach stem intersect the principal shock at the confluence may be expressed as

$$U_{sm} \sin(\alpha - \phi) = U_{s_1} \sin(\theta - \varphi) . \quad (15)$$

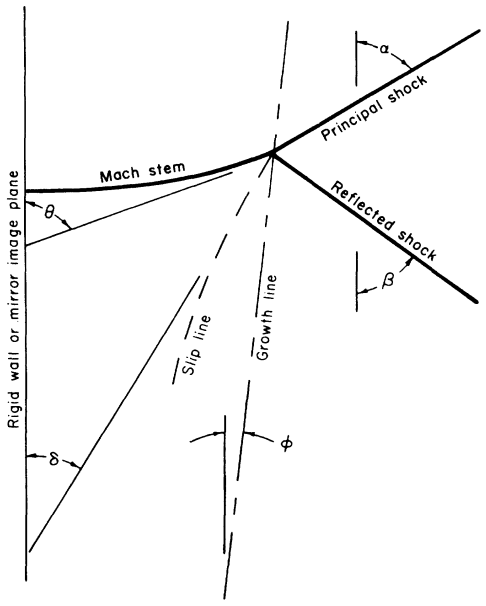

FIG. 3. Schematic of Mach reflection. Shocks are indicated with heavy solid lines. Growth line describes the path of the confluence of the stem, the principal shock, the reflected shock, and a slip line.

The subscript m will refer to the Mach stem shock in the immediate vicinity of the shock confluence. The material which flows through the Mach stem and moves along the slip line is deflected at an angle $\delta-\phi$ described by

$$\tan(\delta-\phi)=\frac{u_{pm}\sin(\theta-\phi)\cos(\theta-\phi)}{U_{sm}-u_{pm}\sin^2(\theta-\phi)} . \quad (16)$$

In the modified model the reflected shock is treated as a disturbance and its shock velocity described by

$$U_{s_2}=\frac{U_{s_1}-u_{p_1}\sin^2(\alpha-\phi)}{\sin(\alpha-\phi)\sin(\beta+\phi)} . \quad (17)$$

The flow which passes through both the incident and reflected shocks and then moves along the slip line is finally deflected at an angle described by

$$\tan(\delta-\varphi)=\frac{u_{p_1}\cos(\alpha-\phi)-u_{p_2}\cos(\beta+\phi)}{(U_{s_2}-u_{p_2})\sin(\beta+\phi)} . \quad (18)$$

The flow model solution is begun by noting that the flow deflections given by Eqs. (16) and (18) are parallel to the slip plane and hence identical. In addition, there is no pressure differential across a slip line. Thus the material which passed through the Mach stem shock must be at the same pressure as that which has come through the principal and reflected shocks. In an experiment, the strength of the incident shock and the incident angle α can usually be established. If the growth angle ϕ and either β, the angle of the reflected shock, or θ, the angle of the Mach stem, are measured, there are sufficient conditions to look for a solution.

The number of Mach reflection experiments reported for solids is extremely limited. In one experimental technique, cameras were used to observe the emergence of the Mach stem at a free surface in an attempt to determine the angles θ and ϕ. In the other, radiography was used to measure β and ϕ directly. In principle, the stem angle θ could also be measured directly with radiographic techniques but lack of resolution has so far precluded the required precision. Three cases of Mach reflection in aluminum or an aluminum alloy will be discussed. An experiment performed by Al'tshuler *et al.*[10] with camera techniques used flying plates to achieve a pressure of 425 GPa behind the Mach stem and reflected shocks. A subsequent radiographic experiment performed by the present author used direct explosive drive to attain 84 GPa. Another radiographic experiment on 2024 aluminum achieved 49 GPa by means of lateral explosive drive. Since this latter experiment has not been previously reported and since it is representative of a general technique, it will be described here.

Two 51-mm wide blocks of the explosive Composition B-3, which sandwich a 25-mm slab of aluminum between them, were detonated on the bottom by a plane-wave lens. A schematic of the experiment is presented in Fig. 4. The aluminum was stepped up so it was not driven directly by the lens. The explosive columns drive two shocks obliquely into the sample. These intersect to form Mach reflection. After the detonation waves have run approximately 100 mm, the 102-mm thick sample is radiographed. The strength of the incident shock is determined by measuring the detonation velocity, observing the angle of the principal

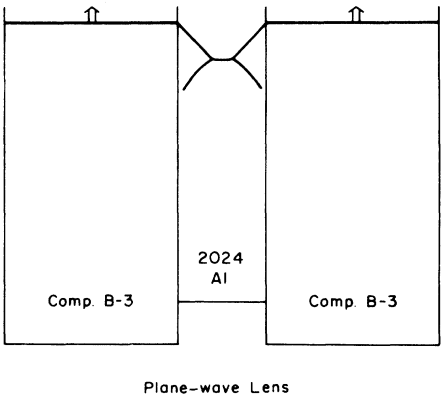

FIG. 4. Schematic of a Mach reflection experiment in which the principal shocks are created by direct perpendicular explosive drive. Small double arrows indicate the direction of motion of the detonation waves.

TABLE III. Mach reflection experiments.

ρ_0 (Mg/m^3)	2.71	2.71	2.785
C_0 (km/sec)	... [a]	5.222	5.328
S_0	... [a]	1.428	1.332
U_{s_1} (km/sec)	...	...	6.39 ± 0.01
ρ_0/ρ_1	...	0.805 ± 0.004	...
P_1 (GPa)	97	27.7 ± 1.0	14.1 ± 0.2
α (deg)	45	50.00	53.80 ± 0.13
ϕ (deg)	9.3 ± 0.5	2.21 ± 0.38	2.46 ± 0.49
β (deg)	...	65.22 ± 1.50	66.10 ± 0.80
θ (deg)	90	...	...
Solution to modified three-shock model			
β (deg)	68.1	...	...
θ (deg)	...	87.6	89.8
U_{s_2} (km/sec)	15.8	9.45 ± 0.12	8.12 ± 0.06
u_{p_2} (km/sec)	4.95	1.75 ± 0.05	1.34 ± 0.05
V_2 (m^3/Mg)	0.165	0.242 ± 0.002	0.262 ± 0.002
P_2' (GPa) P_m (GPa)	425	83.5 ± 2.7	48.8 ± 1.3
$\gamma(V_2)$	0.87 (± 0.05) (1.2) [b]	1.66 ± 0.14	1.38 ± 0.23

[a] The Soviet Hugoniot is not represented as a linear relation between shock and particle velocities. See Ref. 10.

[b] Value with thermal electron contributions removed.

shock, and hence deducing the shock velocity in the sample.

The results of all three experiments are listed in Table III in the order mentioned. The upper portion of the table lists the parameters for the incident shock which were either measured directly or determined from the principal Hugoniot. The lower portion lists those angles and other quantities obtained by the solution of the modified three-shock model. In actual practice Eq. (17) was used for the last two experiments to evaluate the velocity of the reflected shock. The equivalency of the Mach stem pressure with the pressure behind the reflected shock, as given by Eq. (7), permits the particle velocity for the reflected shock to be written

$$u_{p_2} = V_1(\rho_0 u_{pm} U_{sm} - P_1)/U_{s_2} = F(\theta - \phi) . \tag{19}$$

The right-hand side of this equation is a function of $\theta - \phi$ through the condition in Eq. (15) and the fact that the material state behind the Mach stem shock is on the principal Hugoniot. The equivalency of flow deflection provides a second relationship. With appropriate substitutions from the above expression, the deflection can be written

$$\tan(\theta - \phi) = \frac{(P_1 + u_{p_2} U_{s_2}/V_1)(U_{s_2} - u_{p_2}) \sin(\beta + \phi)}{[\rho_0 U_{s_1}^2 \sin^{-2}(\alpha - \phi) - P_1 - u_{p_2} U_{s_2}/V_1][u_{p_1} \cos(\alpha - \phi) - u_{p_2} \cos(\beta + \phi)]} = f(u_{p_2}) . \tag{20}$$

In this case the right-hand side is a function only of u_{p_2} and the two equations can be solved simultaneously to yield the results listed in the bottom half of the last two columns of Table III. In Al'tshuler's experiment the angle θ was measured instead of β. In that case all the parameters for the Mach stem shock can be determined immediately from Eq. (15) and the principal Hugoniot and the flow deflection is given by Eq. (16). The remaining equations can then be solved in the form

$$\sin(2\beta + \phi + \delta) = \sin(\delta - \phi) - 2\cos(\delta - \phi) \times \frac{A[A \tan(\delta - \phi) - u_{p_1} \sin(\alpha - \phi) \cos(\alpha - \phi)]}{V_1(P_m - P_1) \sin^2(\alpha - \phi)} , \tag{21}$$

where

$$A = U_{s_1} - u_{p_1} \sin^2(\alpha - \phi) . \tag{22}$$

Once this expression is solved for β, the velocities associated with the reflected shocks are given by Eqs. (17) and (19). The standard deviation for γ listed in parentheses is again based on an estimate of the minimum errors likely to occur in such an experiment.

A graphical representation of the final solution for Al'tshuler's experiment is presented in Fig. 5. The dashed line indicates the pressures and flow deflections permitted by the principal Hugoniot for material which passes through the Mach stem near the confluence. The locations of various values of θ are indicated. The solution for the flow which emerges from the reflected shock is shown as a solid line. Its exact location in this plane depends on the values and functional forms used for γ. The value which permits it to intersect the dashed curve at the measured value of θ gives the solution to the model.

For pressures of the magnitude achieved in this experiment, the contributions to the pressure and energy from the thermally excited electrons are no longer insignificant compared to those from lattice compression. Consequently the magnitude of this effect has been estimated using a method discussed by Al'tshuler. Details are included in the Appendix. The value of γ due to lattice vibrations alone is enclosed in parentheses at the bottom of Table III.

The analysis of Mach reflection experiments, at least for the experimental techniques used thus

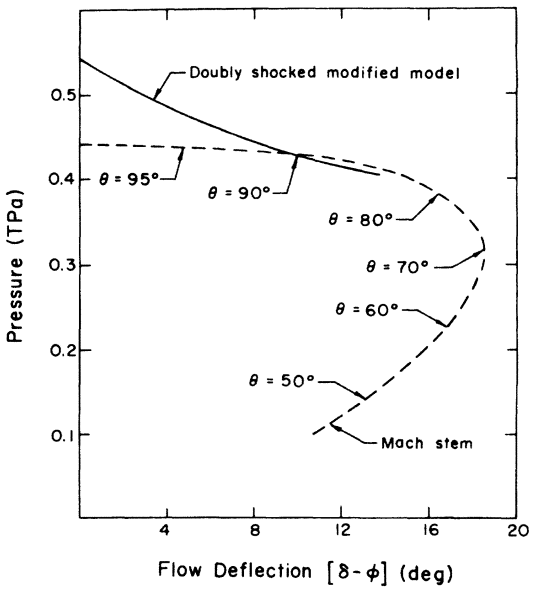

FIG. 5. Graphical representation of the flow solution for the modified three-shock model with a slip line. This particular solution is for the Mach reflection experiment of Al'tshuler *et al*. (Ref. 10).

far, depends on some model of the flow. This small drawback is considered to be outweighed by the multiplication of incident pressure that can be achieved behind the reflected shock. The compression achieved behind the reflected shock in Al'tshuler's experiment corresponds to a pressure on the principal Hugoniot slightly over six times the incident pressure. Furthermore, the precision exhibited in Table III appears to be on a par with that obtained in regular reflection.

V. POROUS SAMPLES

Another method of determining the Grüneisen coefficient involves the acquisition of Hugoniot information for samples with below-standard densities. When such samples are shock compressed some energy is needed to collapse the voids, so the total energy needed to compress to a given volume is much greater than for nonporous samples. The extra energy appears as thermal energy and results in a higher pressure than the corresponding state on the principal Hugoniot. This larger pressure and energy can be used directly in Eq. (1) to evaluate γ. Since aluminum is used as an impedance-match reference material in shock-wave work, this particular problem has received a great deal of attention. Kormer *et al.*[11] have published some results for porous aluminum, and the Shock Wave Physics Group at Los Alamos has performed over a hundred Hugoniot experiments on porous 2024 aluminum.[12,13] The work on 2024 will be used here, since it is more extensive. Experimental Hugoniots were determined for four different porosities of 2024 aluminum. The higher-pressure results for porous samples appear to be reasonably linear in the shock-velocity–particle-velocity plane, although the lower-pressure results exhibit a good deal of curvature. When comparing shocked porous material with shocked standard material it is desirable that the voids be sufficiently collapsed that the material structures are similar. Thus lower-pressure data should probably be avoided when evaluating γ. Consequently, linear representations are probably adequate for this discussion, and my fits to the remaining data are listed in Table IV. The pressure range refers to fit pressures for the experimental results used. To determine the Grüneisen coefficient, the principal Hugoniot will serve as the master reference, as it has throughout this paper, since the experiments which determine it are more numerous and more precise. The results for γ from the Hugoniots centered at below-standard densities are presented in Fig. 6 as solid lines. The lines are labeled according to the initial porous density. The use of linear U_s-u_p fits imposes a specific functional form on γ. Thus γ has only been evaluated over the range of volumes for which experimental results exist and are adequately described by such a fit. Error bars representing standard deviations are included at both ends of the result for a particular density. These errors arise from the scatter in the Hugoniot data for porous samples. When making linear fits to these results, small variations in initial density were corrected by means of the Mie-Grüneisen equation and a self-consistent formulation for γ, that is, the result shown. In general, the standard deviations for γ get smaller as the initial density of the porous material gets smaller and the thermodynamic states achieved get farther off the principal Hugoniot. For the material with the greatest initial porosity, the results for γ near normal solid density are higher than the thermodynamic value indicated by a square. This difference is possibly due to the fact that the porous sample, as a result of shock heating, is above the melting tempera-

TABLE IV. Hugoniots for porous 2024 aluminum.

$\hat{\rho}_0$	C_0 (km/sec)	S_0	Pressure range (GPa)
2.560	4.378	1.438	$31 < P < 104$
2.227	3.024	1.623	$29 < P < 99$
1.955	2.160	1.670	$25 < P < 91$
1.659	1.439	1.685	$17 < P < 89$

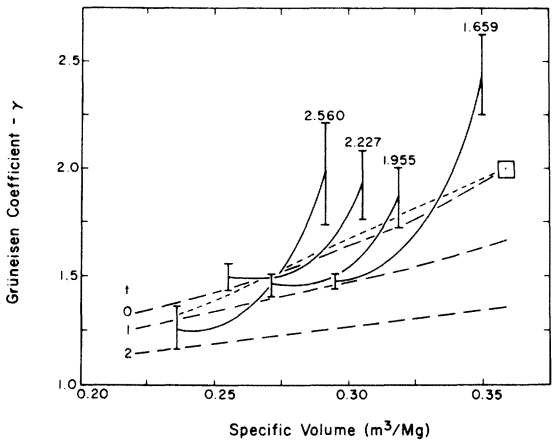

FIG. 6. Experimental results from porous samples and popular functional formulations for the Grüneisen coefficient of 2024 aluminum. Solid lines are from Hugoniots centered on the densities listed. Dashed lines labeled $t = 0$, 1, and 2 correspond, respectively, to the Slater theory, the Dudgdale-MacDonald theory, and the free-volume theory. Dotted line represents the empirical form where γ/V is a constant. Square is the thermodynamic value.

ture, whereas the material described by the standard reference Hugoniot is still a solid at that volume. Grover[14] has described how a Grüneisen coefficient evaluated from Eq. (1) can exceed the Grüneisen coefficient for the solid if the higher-temperature state used to evaluate γ is immediately above the melting line. A similar effect is also discernible in the results for the other initial porosities.

Included in Fig. 6 for comparison are several forms for γ commonly used in shock work. The dashed lines are given by

$$\gamma(V_1) = \frac{t-2}{3} - \frac{V_1}{2}\,\frac{d^2(P_1V_1^{2t/3})}{dV_1^2}\Big/\frac{d(P_1V_1^{2t/3})}{dV_1} \quad (23)$$

as applied to the 2024-aluminum zero-degree isotherm. The value $t=0$ corresponds to the Slater theory, $t=1$ corresponds to the Dugdale-MacDonald theory, and $t=2$ corresponds to the free-volume theory. Although $t=1$ is useful for many metals, for aluminum it does not agree with the thermodynamic value. The dotted line is the simple form

$$\gamma(V_1)/V_1 = \gamma(V_0)/V_0\,, \quad (24)$$

which is often used in shock work. In this case, where it is chosen to pass through the thermodynamic value, it and the Slater theory seem to best represent the results for porous materials.

VI. CONCLUSIONS

The determinations of the Grüneisen coefficient from the sound speed and Mach and regular reflection experiments discussed in this paper are displayed in Fig. 7. The thermodynamic values for aluminum and the alloy 2024 are also shown. The dashed line represents the conclusion of Kormer *et al.*[11] from their limited data on porous materials. The solid line represents the experiments discussed in this paper. It was established by weighed least-squares segmented fits. All the data discussed for porous materials were included by taking each experiment into account via the porous Hugoniot fits, but the restriction was imposed that the fit pass through the average thermodynamic result with the slope obtained from acoustic experiments.[15] The fit was also not permitted to oscillate unreasonably between the results for the highest two compressions. This final result is also listed numerically in Table V.

States far off the principal Hugoniot are difficult to achieve dynamically for small shock-induced compressions. In consequence, the Grüneisen coefficient cannot be obtained with much precision at such volumes. Shock-compression experiments on porous samples solve this problem to some extent, but for low compressions the possibility of the porous material being melted while the reference material is still solid can introduce additional complications. No static compression work[16] has been discussed in this report, but the behavior in the low-compression region may eventually be resolved through comparison of the isotherm with the principal Hugoniot. At intermediate compressions, a comparison of measurements on second shocks with results from porous materials raises an interesting possibility. Second shock states lie on the cold side of the principal Hugoniot while states attained by singly shocking porous materials lie on the hot side. If both types of measurements are of sufficient accuracy, it may be possible to examine γ for temperature dependence. In the high-compression regime, there is simply a need for more experiments. Both the sound speed measurements and the reflection measurements appear adequate at high pressures. Some results for γ, however, are not completely insensitive to the Hugoniot chosen to analyze the experiment, although an attempt has been made to

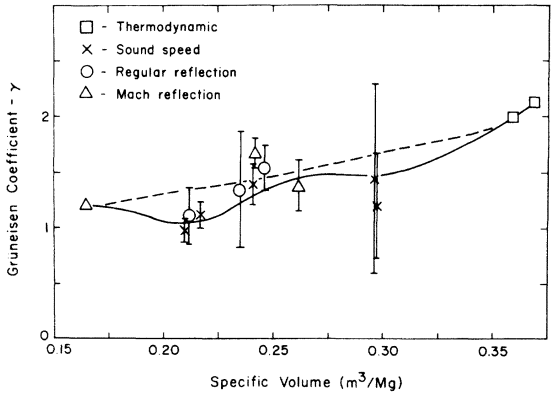

FIG. 7. Results for the Grüneisen coefficient. Thermodynamic values and data from sound speed and reflection experiments are indicated. Dashed line represents the conclusion of Kormer *et al.* (Ref. 11) from their limited experiments on porous samples. Solid line represents a weighted fit to all the results discussed in this paper.

TABLE V. Lattice Grüneisen coefficient.

V (m³/Mg)	γ	V (m³/Mg)	γ	V (m³/Mg)	γ
0.37	2.12	0.30	1.48	0.23	1.17
0.36	2.02	0.29	1.48	0.22	1.08
0.35	1.91	0.28	1.48	0.21	1.03
0.34	1.79	0.27	1.48	0.20	1.05
0.33	1.68	0.26	1.45	0.19	1.12
0.32	1.60	0.25	1.38	0.18	1.18
0.31	1.53	0.24	1.28	0.17	1.20

preserve some sort of self-consistency by using a Hugoniot appropriate to the particular experimenter. Thus hand-in-hand with off-the-principal-Hugoniot experiments, there is a need to continually refine principal Hugoniot references.

ACKNOWLEDGMENT

The author is grateful to the Shock Wave Physics Group of the Los Alamos Scientific Laboratory for permitting him to use their raw data on porous samples.

APPENDIX

The electron contribution to the thermal energy has been represented as[2,4,17]

$$E_e = \tfrac{1}{2}\beta T^2 , \tag{A1}$$

where β, a coefficient that can be obtained from the electronic specific heat, depends principally on volume and can be evaluated from low-temperature experiments at ambient pressure. The corresponding pressure is given by

$$P_e = \gamma_e \beta T^2 / 2V , \tag{A2}$$

where γ_e is the electron analog of the Grüneisen coefficient for the lattice. Dynamic experiments have revealed that the quantum statistical value of $\gamma_e = \frac{1}{2}$ adequately describes aluminum.[2] The determination of electronic contributions thus reduces to a calculation of temperature along the principal and second Hugoniots. In the case of Al'tshuler's Mach reflection experiment, the temperatures were obtained from the high-temperature equation of state for aluminum developed by Naumann.[18] The value of the Grüneisen coefficient which corresponds to the lattice was then determined from Eq. (1) by using only the pressures and energies associated with the lattice compression. The temperature of the material behind the reflected shock was estimated to be 9000°K. This was much less than 33 000°K estimated temperature of a thermodynamic state on the principal Hugoniot at the same compression.

---

†Work performed under the auspices of the Energy Research and Development Administration.

[1] D. J. Pastine and M. J. Carroll in *Accurate Characterization of the High-Pressure Environment*, edited by E. C. Lloyd, NBS Special Publ. 326 (U. S. GPO, Washington, D. C., 1971), pp. 91–104.

[2] L. V. Al'tshuler, Usp. Fiz. Nauk. 85, 197 (1965) [Sov. Phys.-Usp. 8, 52 (1965)].

[3] P. A. Urtiew, J. Appl. Phys. 40, 3962 (1969).

[4] L. V. Al'tshuler, S. B. Kormer, M. I. Brazhnik, L. A. Vladimirov, M. P. Speranskaya, and A. I. Funtikov, Zh. Eksp. Teor. Fiz. 38, 1061 (1960) [Sov. Phys.-JETP 11, 766 (1960)].

[5] G. R. Fowles, J. Appl. Phys. 31, 655 (1960).

[6] D. R. Curran, J. Appl. Phys. 34, 2677 (1963).

[7] T. Neal, J. Appl. Phys. 46, 2521 (1975).

[8] L. V. Al'tshuler and A. P. Petrunin, Zh. Tekh. Fiz. 31, 717 (1961) [Sov. Phys.-Tech. Phys. 6, 516 (1961)].

[9] D. Venable, Phys. Today 17, 19 (1964).

[10] L. V. Al'tshuler, S. B. Kormer, A. A. Bakanova, A. P. Petrunin, A. I. Funtikov, and A. A. Gibkin, Zh. Eksp. Teor. Fiz. 41, 1382 (1961) [Sov. Phys.-JETP 14, 986 (1962)].

[11] S. B. Kormer, A. I. Funtikov, V. D. Urlin, and A. N. Kolesnikova, Zh. Eksp. Teor. Fiz. 42, 686 (1962) [Sov. Phys.-JETP 15, 477 (1962)].

[12] R. G. McQueen, S. P. Marsh, J. W. Taylor, J. N. Fritz, and W. J. Carter, in *High-Velocity Impact Phenomena*, edited by R. Kinslow (Academic, New York, 1970), Chap. 7.

[13] W. J. Carter, S. P. Marsh, J. N. Fritz, and R. G. McQueen, in Ref. 1, pp. 147–158; R. G. McQueen, S. P. Marsh, and W. J. Carter, Los Alamos Scientific Laboratory Report LA-DC-8410 (1965) (unpublished).

[14] R. Grover, J. Chem. Phys. 55, 3435 (1971).

[15] A. C. Holt and R. Grover, in Ref. 1, pp. 131–135.

[16] N. Roy and E. Steward, Nature 224, 905 (1969).

[17] D. E. Rehfuss, J. Appl. Phys. 45, 2530 (1974).

[18] R. J. Naumann, J. Appl. Phys. 42, 4945 (1971); NASA Report TN D-5892 (Federal Scientific and Technical Information Clearinghouse, Washington, D. C., 1971) (unpublished).